Journal of Organometallic Chemistry, 395 (1990) 47–53
Elsevier Sequoia S.A., Lausanne
JOM 21030

Reactivity of pentamethylcyclopentadienyltetrachloromolybdenum(V). Synthesis, structure and electrochemical properties of $[(\eta^5\text{-}C_5Me_5)MoOCl]_2O$

Keisuke Umakoshi and Kiyoshi Isobe *

Department of Applied Molecular Science, Institute for Molecular Science, Myodaiji, Okazaki 444 (Japan)

(Received February 1st, 1990)

Abstract

The reaction of $[(\eta^5\text{-}C_5Me_5)Mo^VCl_4]$ with Na_2WO_4 in THF provides red-brown $[(\eta^5\text{-}C_5Me_5)Mo^VOCl]_2O$, while in water yellow $[(\eta^5\text{-}C_5Me_5)Mo^{VI}O_2]_2O$ is formed. Single-crystal X-ray diffraction analysis has revealed that $[(\eta^5\text{-}C_5Me_5)MoOCl]_2O$ has an anti configuration with a linear Mo–O–Mo skeleton. A cyclic voltammogram of $[(\eta^5\text{-}C_5Me_5)MoOCl]_2O$ in CH_2Cl_2 shows both a reversible and an irreversible two-electron process centered at -0.70 V and $+1.03$ V vs Ag/AgCl, respectively. Crystal data: monoclinic, space group $P2_1/n$, a 10.621(1), b 14.371(3), c 7.689(1) Å, β 93.24(2)°, $Z = 2$.

Introduction

Rhodium and iridium halogeno-complexes with the η^5-pentamethylcyclopentadienyl ligand have a potential affinity to the oxygen atom in oxometalates, and they can be utilized in building organometallic oxide clusters such as $[(\eta^5\text{-}C_5Me_5)MMoO_4]_4$ and $[((\eta^5\text{-}C_5Me_5)M)_4V_6O_{19}]$ (M = Rh and Ir) which have recently been prepared by our group [1]. The corresponding molybdenum complexes, especially tetrahalogeno-compounds $[(\eta^5\text{-}C_5R_5)MoX_4]$ (R = H, Me; X = halide) are much more oxophilic and versatile starting materials [2–4]. In the course of our study on the reaction of $[(\eta^5\text{-}C_5Me_5)MoCl_4]$ with Na_2WO_4 in THF, we identified the formation of a new μ-oxo-bis[(η^5-pentamethylcyclopentadienyl)chlorooxomolybdenum] complex, $[(\eta^5\text{-}C_5Me_5)MoOCl]_2O$. This paper describes the structure and electrochemistry of $[(\eta^5\text{-}C_5Me_5)MoOCl]_2O$, as well as some reactivities of $[(\eta^5\text{-}C_5Me_5)MoCl_4]$.

Results and discussion

Reaction of $[(\eta^5\text{-}C_5Me_5)MoCl_4]$

The heterogeneous reaction of $[(\eta^5\text{-}C_5Me_5)MoCl_4]$ with anhydrous Na_2WO_4 in THF gave the red-brown complex $[(\eta^5\text{-}C_5Me_5)MoOCl]_2O$ in 36% yield (eq. 1), but

0022-328X/90/$03.50

the use of Na_2MoO_4, $NaVO_3$, or an excess of water in place of Na_2WO_4 did not

$$[(\eta^5\text{-}C_5Me_5)MoCl_4] + Na_2WO_4 \xrightarrow[\text{in THF}]{} [(\eta^5\text{-}C_5Me_5)MoOCl]_2O \qquad (1)$$

produce $[(\eta^5\text{-}C_5Me_5)MoOCl]_2O$. Addition of 1.5 equivalent amounts of water to a suspension of $[(\eta^5\text{-}C_5Me_5)MoCl_4]$ in THF led to the formation of a dark-orange solution whose absorption spectrum corresponded to that of $[(\eta^5\text{-}C_5Me_5)MoOCl]_2O$, and a dark-red solid was obtained on evaporation of the solvent. This solid, however, was presumed to be $[(\eta^5\text{-}C_5Me_5)MoCl_2(OH)]_2O$, by analogy with the reaction of $[(\eta^5\text{-}C_5Me_5)TaCl_4]$ with water [5], and from the results of elemental analysis. Thereupon, 3.2 equivalent amounts of Proton Sponge ($C_{10}H_6(N(CH_3)_2)_2$), Na_2MoO_4, $NaVO_3$, or Na_2WO_4 were added to the dark-orange solution to trap any HCl generated. The addition of the first three led to a color change to a greenish solution and did not give $[(\eta^5\text{-}C_5Me_5)MoOCl]_2O$, while the addition of the last produced it in almost the same yield as under anhydrous conditions. Thus the results show that isolation of $[(\eta^5\text{-}C_5Me_5)MoOCl]_2O$ from the dark-orange solution may need an appropriate base. $[(\eta^5\text{-}C_5Me_5)MoOCl]_2O$ is very air-sensitive in dichloromethane, giving $[(\eta^5\text{-}C_5Me_5)MoO_2Cl]$ and blue decomposition products (eq. 2). Similar blue decomposition products were isolated by the hydrolysis of $[(\eta^5\text{-}C_5H_5)MoCl_4]$ in an open flask [2].

$$[(\eta^5\text{-}C_5Me_5)MoOCl]_2O \xrightarrow[\text{in } CH_2Cl_2]{O_2} 2[(\eta^5\text{-}C_5Me_5)MoO_2Cl] \qquad (2)$$

On the other hand, the reaction of $[(\eta^5\text{-}C_5Me_5)MoCl_4]$ with Na_2MoO_4, Na_2WO_4 or $NaVO_3$ in water gave the yellow $[(\eta^5\text{-}C_5Me_5)MoO_2]_2O$ complex which precipetated from solution by successive acidification (pH ca. 4) with conc. HCl (eq. 3).

$$[(\eta^5\text{-}C_5Me_5)MoCl_4] + Na_xMO_y \xrightarrow[\text{in water}]{} [(\eta^5\text{-}C_5Me_5)MoO_2]_2O \qquad (3)$$

$[(\eta^5\text{-}C_5Me_5)MoO_2]_2O$ is usually obtained as the final product from various reactions, for example the photochemical reaction of $[(\eta^5\text{-}C_5Me_5)Mo(CO)_3]_2$ with $NaNO_2$ [6], the exposure of a solution of $[(\eta^5\text{-}C_5Me_5)Mo(CO)_2]_2$ in chloroform to air [7], the reaction of $[(\eta^5\text{-}C_5Me_5)Mo(Br)(CH_3)(NO)]_2$ with O_2 in sunlight [8], or the oxidation of a suspension of $[((\eta^5\text{-}C_5Me_5)Mo(CO)_2(OMe))n]$ in THF with oxygen [9]. These facts indicate that the $MoO_2\text{–}O\text{–}MoO_2$ skeleton is one of the most stable forms among molybdenum species, although the reaction of $MoCl_5$ with $KHB(pz)_3$ ($HB(pz)_3{}^- =$ hydrotripyrazolylborate) in dilute HCl provides $[HB(pz)_3MoOCl]_2O$ [10], which is an analog of $[(\eta^5\text{-}C_5Me_5)MoOCl]_2O$.

Structural characterization of $[(\eta^5\text{-}C_5Me_5)MoOCl]_2O$

The IR spectrum of $[(\eta^5\text{-}C_5Me_5)MoOCl]_2O$ shows characteristic bands at 959, 933, 910 and 879 cm^{-1} which can be assigned to Mo=O symmetric and asymmetric stretching vibrations, and bands at 721 and 404 cm^{-1} which are due to the Mo–O–Mo asymmetric stretching and the Mo–Cl stretching vibrations, respectively. The ^1H NMR signal of the methyl protons of $[(\eta^5\text{-}C_5Me_5)MoOCl]_2O$ resonates at δ 2.07 as a sharp singlet, which indicates that the two C_5Me_5 rings are magnetically equivalent and that the molecule is diamagnetic owing to spin-pairing by the Mo-Mo interaction, despite the presence of a pentavalent molybdenum ion. An analogous antiferromagnetic interaction was observed in the two geometrical isomers of $[HB(pz)_3MoOCl]_2O$: the C_i isomer, having a crystallographically im-

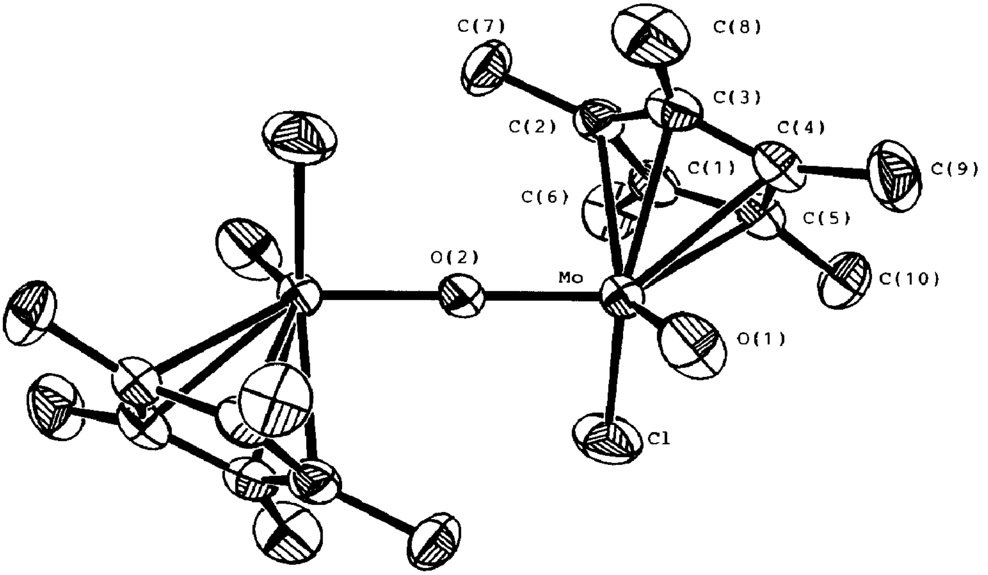

Fig. 1. ORTEP diagram of $[(\eta^5\text{-}C_5Me_5)MoOCl]_2O$. Thermal ellipsoids are drawn at the 50% probability level.

posed center of symmetry, and the C_2 isomer, having no center of symmetry, are both diamagnetic [10]. X-ray structure analysis disclosed that $[(\eta^5\text{-}C_5Me_5)MoOCl]_2O$ is centrosymmetric with an *anti* configuration, having a linear Mo–O–Mo bridge as required by crystal symmetry; the oxo groups as well as the other ligands are *trans* to one another (Fig. 1). Each molybdenum ion has a coordination number of six and is in a pseudooctahedral coordination environment. Atomic coordinates are listed in Table 1. Selected bond lengths and angles are given in Table 2.

Two geometrical isomers in $[HB(pz)_3MoOCl]_2O$ (C_i and C_2) [10] and $[MeCpMo(O)(\mu\text{-}S)]_2$ (*syn* and *anti*) [11] were isolated and characterized by means

Table 1

Positional parameters and isotropic temperature factors for $[(\eta^5\text{-}C_5Me_5)MoOCl]_2O$

Atom	*x*	*y*	*z*	B_{eq}, Å^2
Mo	0.13603(5)	0.06858(4)	0.0973(1)	2.41(1)
Cl	0.0290(2)	0.2113(2)	0.0453(3)	4.8(1)
O(1)	0.1455(5)	0.0511(4)	0.3131(7)	4.6(2)
O(2)	0	0	0	3.2(2)
C(1)	0.2678(6)	0.1068(5)	−0.1397(9)	2.8(2)
C(2)	0.2558(6)	0.0103(5)	−0.1354(9)	2.7(2)
C(3)	0.3114(6)	−0.0215(5)	0.0318(9)	3.0(2)
C(4)	0.3611(6)	0.0580(5)	0.1214(9)	3.1(2)
C(5)	0.3291(6)	0.1380(5)	0.0216(9)	3.0(2)
C(6)	0.2249(8)	0.1702(5)	−0.291(1)	4.0(2)
C(7)	0.1995(7)	−0.0521(5)	−0.2783(9)	3.8(2)
C(8)	0.3250(8)	−0.1218(5)	0.090(1)	4.6(3)
C(9)	0.4310(7)	0.0565(7)	0.302(1)	4.7(2)
C(10)	0.3637(8)	0.2392(5)	0.064(1)	4.2(2)

Table 2

Selected bond distances (Å) and angles (deg) for $[(\eta^5\text{-}C_5Me_5)MoOCl]_2O$

Mo–Cl	2.368(2)	Mo–C(2)	2.403(7)
Mo–O(1)	1.676(5)	Mo–C(3)	2.346(7)
Mo–O(2)	1.870(1)	Mo–C(4)	2.392(6)
Mo–C(1)	2.423(7)	Mo–C(5)	2.382(7)
O(1)–Mo–O(2)	108.6(2)		
O(1)–Mo–Cl	107.4(2)		
O(2)–Mo–Cl	92.1(1)		

of X-ray diffraction. On the other hand, only the *anti* isomer was obtained for $[(\eta^5\text{-}C_5Me_5)MoOCl]_2O$ and $[(\eta^5\text{-}C_5H_5)MoOI]_2O$ [3,12]. This might be attributed to steric requirements around the bridging oxygen atom. The μ-O–Mo distance (1.870(1) Å) is comparable to those of complexes having a linear Mo–O–Mo skeleton (1.856(1) Å in $[(\eta^5\text{-}C_5H_5)MoOI]_2O$, 1.829(4)–1.883(4) Å in $[HB(pz)_3MoOCl]_2O$, and 1.84(1)–1.89(1) Å in $[(\eta^5\text{-}C_5Me_5)MoO_2]_2O$ [7–9]). The Mo=O distance in $[(\eta^5\text{-}C_5Me_5)MoOCl]_2O$ (1.676(5) Å) is similar to those in $[(\eta^5\text{-}C_5H_5)MoOI]_2O$ (1.684(6) Å) and the "C_2 isomer" of the pyrazoylborate complex (1.670(4) and 1.671(4) Å), but shorter than the anomalously long distance in the "C_i isomer" (1.779(6) Å). The Mo–Cl distance in our complex (2.368(3) Å) is close to those in both isomers of the pyrazoylborate complex (2.334(3)–2.364(2) Å). The bond angles of O(1)–Mo–O(2), O(2)–Mo–Cl, and O(1)–Mo–Cl are 108.6°, 92.1°, and 107.4°, respectively, and the structure may be described as a 'double three-legged piano stool'.

Electrochemistry

The cyclic voltammogram of $[(\eta^5\text{-}C_5Me_5)MoOCl]_2O$ is shown in Fig. 2. The compound exhibits an irreversible oxidation process with $E_{pa} = +1.03$ V, a reversible reduction process with $E_{1/2} = -0.70$ V ($\Delta E_p = 90$ mV because of high *iR*-drop) and an irreversible reduction process with $E_{pc} = -1.18$ V. Controlled-potential coulometry for the compound at +1.10 V (vs Ag) gave an electron stoichiometry of 1.9 ± 0.1 e/dimer. The irreversible wave with $E_{pa} = +1.03$ V is a two-electron process and the resulting oxidation product is unstable and rapidly decomposes.

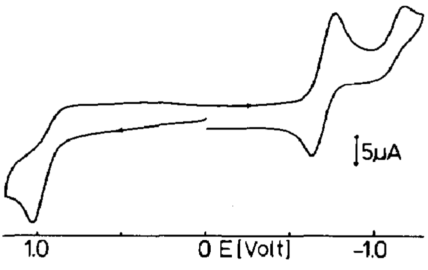

Fig. 2. Cyclic voltammogram of $[(\eta^5\text{-}C_5Me_5)MoOCl]_2O$ in 0.1 *M* TBAP–CH_2Cl_2 at a glassy-carbon electrode with a scan rate of 50 mV s^{-1}.

The electrode reaction for the oxidation process is therefore represented by:

$$[(\eta^5\text{-}C_5Me_5)_2Mo^{V}{}_2O_3Cl_2] \rightleftharpoons [(\eta^5\text{-}C_5Me_5)_2Mo^{VI}{}_2O_3Cl_2] + 2e^-$$

$$[(\eta^5\text{-}C_5Me_5)_2Mo^{VI}{}_2O_3Cl_2] \rightarrow X_1$$

$$(X_1 = \text{decomposition products})$$

Controlled-potential coulometry for the compound at −0.90 V (vs Ag) gave an electron stoichiometry of 1.8 ± 0.1 e/dimer. The reversible wave ($i_{pa}/i_{pc} = 0.88$) in the first reduction process and the small peak current of the irreversible reduction wave in the second process indicate that the rate of the electron-transfer reaction of the second process is sufficiently slow. Unfortunately, we could not determine the electron stoichiometry of the irreversible reduction process because of the instability of potential in the coulometry. The structure of the compound, $[(\eta^5\text{-}C_5Me_5)_2Mo^{V}{}_2O_3Cl_2]$, is retained, at least in the first reduction process. The electrode reaction for the reduction process is represented by:

$$[(\eta^5\text{-}C_5Me_5)_2Mo^{V}{}_2O_3Cl_2] + 2e^- \rightleftharpoons [(\eta^5\text{-}C_5Me_5)_2Mo^{IV}{}_2O_3Cl_2]$$

$$[(\eta^5\text{-}C_5Me_5)_2Mo^{IV}{}_2O_3Cl_2] + ne^- \underset{\text{slow}}{\rightleftharpoons} [(\eta^5\text{-}C_5Me_5)_2Mo^{IV\text{-}n/2}{}_2O_3Cl_2]$$

$$[(\eta^5\text{-}C_5Me_5)_2Mo^{IV\text{-}n/2}{}_2O_3Cl_2] \rightarrow X_2$$

$$(X_2 = \text{decomposition products})$$

Experimental

Air-sensitive materials were handled under argon, unless otherwise stated. $[(\eta^5\text{-}C_5Me_5)MoCl_4]$ was prepared from pentamethylcyclopentadiene (Aldrich), butyllithium (Wako), hexacarbonylmolybdenum (Aldrich), methyliodide (Wako), and phosphorus pentachloride (Wako) by published methods [4,13]. Dichloromethane was redistilled over $CaCl_2$ under an argon atmosphere. Tetrahydrofuran (with benzophenone) and n-hexane were redistilled over sodium under argon before use. Tetrabutylammonium perchlorate (TBAP, Wako) was recrystallized twice from ethanol.

The IR spectra were recorded in Nujol mulls on a Hitachi 270-30 infrared spectrophotometer. The ^1H NMR spectra were taken on a JEOL GX-400 spectrometer with $CDCl_3$ as solvent. UV–VIS spectra were recorded on a Hitachi U-3400 spectrophotometer.

Preparation of $[(\eta^5\text{-}C_5Me_5)MoOCl]_2O$

$[(\eta^5\text{-}C_5Me_5)MoCl_4]$ (250 mg, 0.67 mmol) and anhydrous Na_2WO_4 (400 mg, 1.36 mmol), obtained by heating $Na_2WO_4 \cdot 2H_2O$ in vacuo at 100 °C, were refluxed in THF (40 cm^3) for 48 h with stirring. The color of the suspension gradually changed from purple to orange during reflux. After the removal of unreacted Na_2WO_4, the filtrate was evaporated to dryness to give a dark-orange solid. This was dissolved in 10 cm^3 of dichloromethane and then 2 cm^3 of n-hexane was added to the solution to make the unchanged precipitate $[(\eta^5\text{-}C_5Me_5)MoCl_4]$, which was carefully filtered off, and the filtrate was cooled at −10 °C for 2 days. The dark-orange crystals were washed with hexane; yield: 70 mg (36%). If the removal of unchanged $[(\eta^5\text{-}$

$C_5Me_5)MoCl_4]$ is inadequate, it contaminates $[(\eta^5\text{-}C_5Me_5)MoOCl]_2O$. Anal. Found: C, 40.91; H, 5.19. $C_{20}H_{30}O_3Cl_2Mo_2$ calcd: C, 41.32; H, 5.21%.

Reaction of $[(\eta^5\text{-}C_5Me_5)MoCl_4]$ with Na_2MoO_4, Na_2WO_4 or $NaVO_3$ in water

$[(\eta^5\text{-}C_5Me_5)MoCl_4]$ (250 mg, 0.67 mmol) was suspended in an aqueous solution of Na_xMO_y ($Na_xMO_y = Na_2MoO_4$, Na_2WO_4 or $NaVO_3$, 6.7 mmol/50 cm^3). The suspension was stirred for 10 min at room temperature and turned dark brown. A yellow solid was separated from the solution acidified to pH ca. 4 with hydrochloric acid. Acidification is not necessary for the reaction with $NaVO_3$. The yellow solid was collected, washed with ether, and dried in vacuo; yield: ca. 130 mg (70–75%). This yellow product was characterized by IR spectroscopy and elemental analysis as $[(\eta^5\text{-}C_5Me_5)MoO_2]_2O$, which we had prepared previously [6]. IR: 1071, 1033, 909 (ν_{as} Mo=O), 879 (ν_s Mo=O), 803, 763 (ν_{as} Mo–O–Mo), 619, 547, 432, 404 cm^{-1}. Anal. Found: C, 44.07; H, 5.63. $C_{20}H_{30}O_5Mo_2$ calcd: C, 44.29; H, 5.59%.

Reaction of $[(\eta^5\text{-}C_5Me_5)MoCl_4]$ with water

$[(\eta^5\text{-}C_5Me_5)MoCl_4]$ (250 mg, 0.67 mmol) and water (18.1 mg, 1.01 mmol) were stirred in THF (40 cm^3) at room temperature for 1 h. The solvent was then evaporated to dryness under reduced pressure. The residue was extracted with 10 cm^3 of dichloromethane, and then 2 cm^3 of n-hexane was added to precipitate a dark-red solid. The solid was separated, washed with hexane, and dried in vacuo; yield: 142 mg (65%). Anal. Found: C, 36.75; H, 4.93. $C_{20}H_{32}O_3Cl_4Mo_2$ calcd: C, 36.72; H, 4.94%.

Crystal data of $[(\eta^5\text{-}C_5Me_5)MoOCl]_2O$

A crystal of $[(\eta^5\text{-}C_5Me_5)MoOCl]_2O$ suitable for the X-ray diffraction study was grown from dichloromethane/n-hexane at −10 °C. $C_{20}H_{30}O_3Cl_2Mo_2$, $M = 581.28$, monoclinic, space group $P2_1/n$, a 10.621(1), b 14.371(3), c 7.689(1) Å, β 93.24(2)°, V 1171.8(3) Å^3, D_c 1.65 g cm^{-3}, $Z = 2$, $F(000) = 584$, Mo-K_α radiation ($\lambda = 0.71073$ Å), $\mu(\text{Mo-}K_\alpha) = 12.92$ cm^{-1}.

Intensity data collection and refinements

The crystal was sealed in a thin-walled glass capillary. The cell dimensions were determined from a least-squares treatment of 50 2θ values of higher-angle reflections ($20 \leq 2\theta \leq 30°$) measured on a Rigaku AFC-5 diffractometer by the use of Mo-K_α radiation. Reflections were recorded by the ω–2θ scan technique with a scan range of $1.2 + 0.5°$ tan θ in the range ($2 \leq 2\theta \leq 55°$). Three standard reflections (400, $0\bar{6}0$, $\bar{1}03$) were measured after every 50 reflections, and no significant change in intensities was detected. In a total of 3004 unique reflections collected, 1513 with ($F_o > 3\sigma(F_o)$) were used in further calculations.

Intensities were corrected for Lorentz and polarization effects in the usual manner. Neither absorption nor extinction corrections were made. The crystal structure was solved by the Patterson–Fourier method. The positional and thermal parameters were refined by the block-diagonal-matrix least-squares method. The minimized function was $\Sigma w(|F_o| - |F_c|)^2$, where $w^{-1} = \sigma^2(|F_o|) + (0.015|F_o|)^2$. No attempt was made to locate hydrogen atoms in the structure analysis. Final R values of 0.0356 and $R_w = 0.0511$ were obtained. In the final refinement cycle all parameter shifts were less than 0.1σ. Final difference syntheses showed no peak greater than 0.95 e Å^{-3}.

The atomic scattering factors, corrected for the anomalous dispersion of Mo^0 and Cl^0, were taken from ref. [14]. Computational work was carried out using standard programs in UNICS [15] and ORTEP [16].

Electrochemical measurements

Cyclic voltammetry was performed with a Hokuto HA-501G GPIB potentiostat and a Hokuto HB-105 arbitrary function generator equipped with a Yokogawa 3025 *x–y* recorder. The working and counter electrodes were a glassy carbon disk and a platinum wire, respectively. Cyclic voltammograms of $[(\eta^5\text{-}C_5Me_5)MoOCl]_2O$ and $[(\eta^5\text{-}C_5Me_5)MoO_2]_2O$ were measured in CH_2Cl_2. The Ag/AgCl electrode was used as a reference electrode. The reference electrode was checked periodically against the ferrocenium/ferrocene couple (Fc^+/Fc) in CH_2Cl_2. The half-wave potential of Fc^+/Fc was 0.451 (vs Ag/AgCl) or 0.350 V (vs Ag) ($\Delta E_p = 170$ mV).

Controlled potential coulometry was carried out in a standard H-type cell with a Hokuto HA-501G GPIB potentiostat and a Hokuto HF-201 coulometer. The working electrode was made of platinum gauze and the working compartment was separated from the counter compartment by a sintered glass disk. An Ag wire was used as the reference electrode.

Electrochemical measurements were performed at 25 ± 1 °C. Samples (ca. 2×10^{-6} mol) containing 1×10^{-3} mol TBAP as supporting electrolyte were dissolved in 10 cm^3 of CH_2Cl_2 redistilled under an argon atmosphere. All potentials reported here are relative to the Ag/AgCl reference electrode unless otherwise stated.

Acknowledgement

We gladly acknowledge the award of an IMS fellowship (to K.U.). This work was partly supported by the Joint Studies Program (1989-1990) of the Institute for Molecular Science.

References

1 Y. Hayashi, K. Toriumi and K. Isobe, J. Am. Chem. Soc., 110 (1988) 3666; Y. Hayashi, Y. Ozawa and K. Isobe, Chem. Lett., (1989) 425.
2 M. Cousins and M.L.H. Green, J. Chem. Soc. (A), (1969) 16.
3 M.J. Bunker and M.L.H. Green, J. Chem. Soc., Dalton Trans., (1981) 847.
4 R.C. Murray, L. Blum, A.H. Liu and R.R. Schrock, Organometallics, 4 (1985) 953.
5 P. Jernakoff, C. de Meric de Bellefon, G.L. Geoffroy, A.L. Rheingold and S.J. Geib, Organometallics, 6 (1987) 1362, and references therein.
6 K. Isobe, S. Kimura and Y. Nakamura, J. Organomet. Chem., 331 (1987) 221.
7 J.W. Faller and Y. Ma, J. Organomet. Chem., 340 (1988) 59.
8 P. Gomez-Sal, E. de Jesus, P. Royo, A. Vazquez de Miguel, S. Martinez-Carrera and S. Garcia-Blanco, J. Organomet. Chem., 353 (1988) 191.
9 P. Leoni, M. Pasquali, L. Salsini, C. di Bugno, D. Braga and P. Sabatino, J. Chem. Soc., Dalton Trans., (1989) 155.
10 S. Lincoln and S.A. Koch, Inorg. Chem., 25 (1986) 1594.
11 L.D. Tanner, R.C. Haltiwanger and M.R. DuBois, Inorg. Chem., 27 (1988) 1741.
12 C. Couldwell and C.K. Prout, Acta Crystallogr. B, 1980, 36, 1481.
13 R.B. King and M.B. Bisnette, J. Organomet. Chem., 8 (1967) 287
14 International Tables for X-ray Crystallography; Kynoch Press: Birmingham, England, 1974; Vol. IV.
15 UNICX; Crystallographic Society of Japan, Tokyo, 1969.
16 C.K. Johnson, ORTEP II, Report ORNL-5138; Oak Ridge National Laboratory: Oak Ridge, TN, 1976.